*electronic materials*

MDPI

*Article*

# High Rectification Ratio in Polymer Diode Rectifier through Interface Engineering with Self-Assembled Monolayer

**Khaoula Ferchichi [1,2,*], Sebastien Pecqueur [1], David Guerin [1], Ramzi Bourguiga [2] and Kamal Lmimouni [1]**

[1] Univ. Lille, CNRS, Centrale Lille, Univ. Polytechnique Hauts-de-France, UMR 8520—IEMN—Institut d'Electronique de Microélectronique et de Nanotechnologie, F-59000 Lille, France; sebastien.pecqueur@univ-lille.fr (S.P.); david.guerin@iemn.fr (D.G.); kamal.lmimouni@univ-lille.fr (K.L.)

[2] Laboratoire Physique des Matériaux, Structures et Propriétés Groupe Physique des Composants et Dispositifs Nanométriques, Facultés des sciences de Bizerte, Université de Carthage, Jarzouna-Bizerte 7021, Tunisia; bourguigar@yahoo.fr

* Correspondence: khaoula.ferchichi@univ-lille.fr

**Abstract:** In this work, we demonstrate P3HT (poly 3-hexylthiophene) organic rectifier diode both in rigid and flexible substrate with a rectification ratio up to $10^6$. This performance has been achieved through tuning the work function of gold with a self-assembled monolayer of 2,3,4,5,6-pentafluorobenzenethiol (PFBT). The diode fabricated on flexible paper substrate shows a very good electrical stability under bending tests and the frequency response is estimated at more than 20 MHz which is sufficient for radio frequency identification (RFID) applications. It is also shown that the low operating voltage of this diode can be a real advantage for use in a rectenna for energy harvesting systems. Simulations of the diode structure show that it can be used at GSM and Wi-Fi frequencies if the diode capacitance is reduced to a few pF and its series resistance to a few hundred ohms. Under these conditions, the DC voltages generated by the rectenna can reach a value up to 1 V.

**Keywords:** P3HT; organic diode rectifier; self-assembled monolayer; flexible; energy harvesting; rectenna



**Citation:** Ferchichi, K.; Pecqueur, S.; Guerin, D.; Bourguiga, R.; Lmimouni, K. High Rectification Ratio in Polymer Diode Rectifier through Interface Engineering with Self-Assembled Monolayer. *Electron. Mater.* **2021**, *2*, 445–453. https://doi.org/10.3390/electronicmat2040030

Academic Editor: Heung Cho Ko

Received: 19 July 2021
Accepted: 17 September 2021
Published: 1 October 2021



## 1. Introduction

Nowadays, diode rectifiers are a rapidly growing technology since it can be used in a range of applications such as radio frequency identification (RFID) tags [1], energy harvesting devices [2], and wireless communications [3]. In particular, rectifiers from organic materials have attracted considerable attentions since they offer many advantages of low cost [4], flexibility [1], and soft processing [5].

Among all organic semiconductors, semiconducting polymers allow an excellent physical property of flexibility and easy processability. Among them, poly(3-hexylthiophene) P3HT is one of the most widely benchmarked polymers used in various application fields, such as photovoltaic generators [6,7], photo-sensing diodes [8], organic light-emitting diodes [9,10], p-type transistors [11,12], thermoelectric generators [13,14], synaptic elements [15,16], and also organic diode rectifier [17–21].

Interface properties between electrodes and semiconducting materials play an important role to improve the performance of electronic devices. To achieve good hole injection within the organic semi-conductor layer, it is necessary to diminish the energetic difference between the electrode work-function and the organic semiconductor's highest-occupied molecular orbital (HOMO). Even with the right choice of electrode material matching perfectly the semiconductor's HOMO level, molecular dipole forming at the interface can yield non-negligible energetic barriers for hole injection [22,23]. Many strategies have been investigated in the literature to decrease such injection barriers [18,24,25].

One major approach that has been employed to tune the metal work function is via the functionalization of a self-assembled monolayer (SAM) of molecules that bear large

dipole moment when aligned and functionalized on a surface [26–30]. In particular, SAM of fluorinated thiols has attracted a lot of attention [26,28,31,32]. In addition to their ability to tune metals' work function and improve the charge injection, they can also improve conduction by affecting the molecular packing and crystallinity of organic semiconductors that are deposited either by vacuum evaporation [33], or from solution [34,35]. From molecules that has been widely used, 2,3,4,5,6-pentafluorobenzenethiol (PFBT) shows improved hole injection performances for a large range of applications such as organic field effect transistors (OFET) [26,27,36–39], solar cells [31], memory devices [32,40], and diode rectifier [24,28]. Recently, Chang-mo Kang and coworkers have investigated the effect of these molecules on pentacene-based diodes and high rectification ratio of up to r = $10^7$ has been obtained, with the ability to work in gigahertz frequency range [28].

In this work, we investigate the effect of interface engineering with PFBT SAM in P3HT polymer diode rectifier on rigid and paper substrate. We use this strategy to increase the imbalance between the forward and reverse current of the diode and thus to improve the rectification ratio. The diode is fabricated on a release paper and can be transferred on any other flexible substrate.

By reducing the thickness of the active layer of the diodes, we were also able to reduce the threshold voltages, which allows the diode to be sensitive to very low voltages of the ambient electromagnetic waves in energy harvesting applications.

## 2. Experimental

N type Si wafer (doped with phosphor, 380–400 µm thick, resistivity of 0.0001–0.0003 Ω·cm) with 200 nm thermal oxide layer was used as substrate. The substrate was ultrasonically cleaned with acetone and isopropanol for 10 min each, and then treated by ultra-violet ozone for 25 min to remove any residual contaminants on the surface. With a 5 nm titanium adhesion layer, 120 nm Au were deposited by thermal evaporation through shadow mask to serve as anode contact. For SAM functionalization on the anode, samples were immersed in the solution of 10 µL of PFBT (Sigma-Aldrich, Saint Louis, MO, USA, purity 97%, molecular weight $M_n$ = 15–45 kDA, polydispersity PDI $\leq$ 2) diluted in 10 mL of ethanol for 18 h, and followed by rinsing with pure ethanol and drying under nitrogen flow. After functionalization, the semiconductor was wet-deposited. The solution was prepared by dissolving 30 mg/mL of regioregular P3HT (Sigma-Aldrich 99.995%) in chlorobenzene, and coated in a glove box under a $N_2$ atmosphere at 1000 rpm for 30 s. The thickness was measured by profilometry to be 110 nm. The film was then backed for 1 h at 100 °C in vacuum to remove the remaining solvent. After the deposition of the semiconductor layer, 120 nm of Al was thermally evaporated through shadow mask to form top contacts. The overlap between Au and Al contacts defines the diodes' active area, ranging from $10^{-4}$ to $10^{-2}$ $cm^2$. One sample of P3HT diode without PFBT treatment was fabricated as a reference.

Current–voltage characteristics were measured in a nitrogen-filled glove box ($O_2$ and $H_2O$ < 0.1 ppm) by using a microprobe station connected to an Agilent 4156C parameter analyzer (Keysight Technology, Ulis, France). The forward biasing is corresponding to a positive voltage at the Au electrode with respect to the grounded Al one. AFM was used to analyze the thin-film surface morphology. The modification of Au induced by PFBT was analyzed by contact angle measurement and X-ray photoelectron spectroscopy (XPS) (5600, Physical electronics GmBH, Feldkirchen, Germany). XPS analysis was performed by Physical Electronics system type 5600, under ultra-high vacuum, and by irradiating the surface by a beam of X-rays with a helium discharge lamp with an energy of 21.2 eV. Data were treated using the Multipak software (9.3, UlVAC-PHI, Chigasaki, Kanagawa, Japan).

AFM was performed on Bruker's (Dimension 3100, Santa Barbara, CA, USA), with employing silicon cantilevers (Bruker NCHV-A) in tapping mode with a spring constant of 40 N/m and a resonance frequency of 316 kHz: data were treated using the software Gwyddion.

## 3. Results and Discussion

The structure of the diode is shown in Figure 1a. The effect of PFBT was evaluated by mean of contact angle as shown in Figure 1b,c, and shows a decreased hydrophilicity with PFBT functionalization (θ = 87° compared to 50° for bare gold). Contact angle has been also performed on PFBT-treated Au after a backing at 100 °C for one hour where the measure do not show a significant change (θ = 89°). The later suggests that the temperature does not alter the formation of the monolayer. As the SAM treatment could affect the morphology of the semiconducting layer, AFM microscopy on both surfaces was measured as shown in Figure 1f,g. The PFBT treatment reduced also the roughness of the surface by a factor of 3, it has a value of 7.43 nm on Au surface and was lowered to a value of 2.27 nm with PFBT functionalization. Excess thiol potentially fills the voids on the evaporated Au nanostructured surface, it is worth highlighting that residual SAM molecules remaining at the surface as nanopuddles would have a rather detrimental effect on the current injection [41,42]. XPS spectroscopy was used to analyze the surface composition and further investigate the formation of PFBT on the Au surface as shown in Figure 1c. This spectrum shows a clear peak at 686.4 eV and a peak at 162.4 eV associated respectively to F1s and S2p, a clear signature of PFBT molecules, indicating that the PFBT monolayer is well deposited on gold.

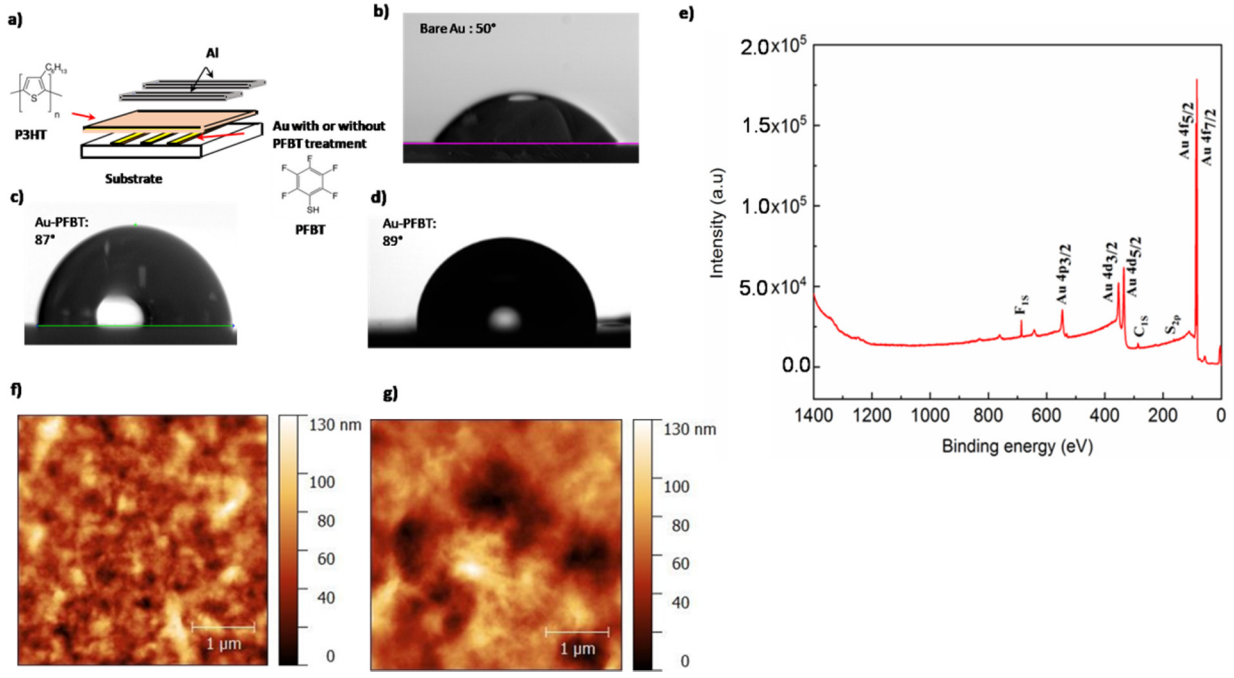


**Figure 1.** (**a**) Schematic structure of a P3HT diode with a PFBT-coated Au anode, (**b**) image of contact angle on bare Au surface, (**c**) image of contact angle on PFBT coated Au surface, (**d**) image of contact angle on PFBT coated Au surface after baking at 100 °C for 1 h, (**e**) XPS analysis of PFBT-modified surface, (**f**) AFM of the P3HT-deposited Au surface, and (**g**) AFM of the P3HT deposited on the modified surface.

### *3.1. Diode Rectifier on Silicon Substrate*

Current-density–voltage (J-V) characteristics of P3HT diode rectifiers with and without PFBT are shown in Figure 2a. The current density is about 0.1 A/cm$^2$ at 4 V for the diode with PFBT one order of magnitude higher than the diode without PFBT. We can also evaluate from this figure the rectification ratio r defined as the ratio between ON and OFF currents at a fixed voltage. r was measured for 13 devices as presented in the histogram of Figure 2b. The rectification ratio r reaches $10^6$ at ±4 V for P3HT diodes with PFBT and spreads from $10^2$ to $10^6$ without SAM functionalization. Few diodes without SAM shows slightly higher rectification, but only due to the particularity low noise current

under reversed polarization, but it is clear from the figure that the SAM treatment leads to increased ON/OFF ratio averagely for all the population of diodes. These values are two orders of magnitude higher than previously obtained for the same rectifying device stack [17–19]. In addition, we can see from these figures, that the diodes with PFBT monolayer are more reproducible. The turn on voltage is defined as the voltage when charge injection is taking place [28] and the current increases gradually, which is about 0.1 V.

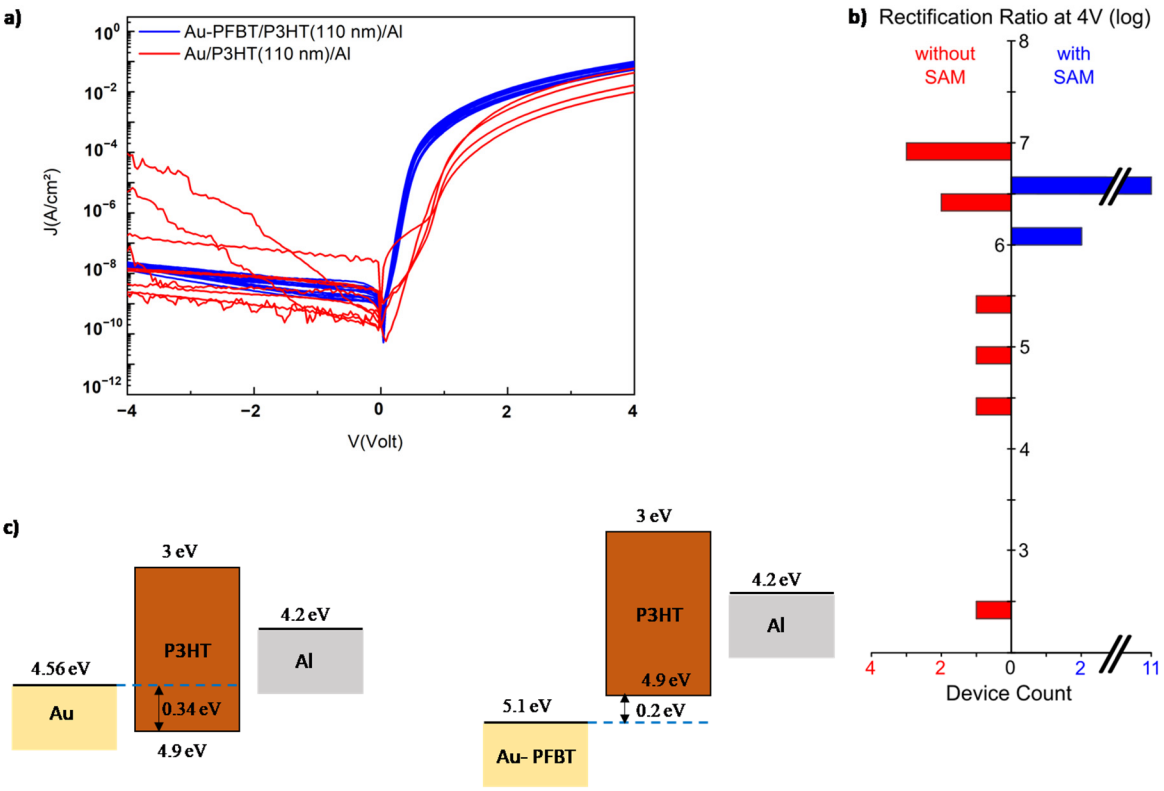


**Figure 2.** (**a**) J-V characteristics of diodes with and without PFBT functionalization, (**b**) rectification ratio collected from 13 diodes, (**c**) energy band diagram of the device [18,43].

This performance improvement can be attributed to two different properties for the PFBT treatment: a first one is the energy barrier reduction between gold and HOMO level of organic semiconductor and the second one is a change in the semiconductor film morphology and molecular orientation. As it has been reported in the literature [32,44,45], the adsorption of PFBT monolayer on gold surface leads to interface dipole layers oriented downward to the metal substrate. Consequently, the work-function of gold increases that value to about 5.1 eV compared to 4.56 eV for untreated gold [43]. From the energy band diagram in Figure 2c, we can see that without PFBT modification, the barrier hole injection has a value of 0.34 eV, and decreases to 0.2 eV with the PFBT, (the value of HOMO and lowest unoccupied molecular orbital (LUMO) are taken from ref [18]). These confirm the reduction of the hole injection barrier and explains the increase of the ON current with PFBT modification.

In addition to tuning the work-function of gold, PFBT also affects the morphological properties of the film and the interface properties as shown in Figure 1. It has been reported in the literature that higher contact angle leads to enhanced crystallinity in the semiconductor and improved mobility near the electrodes [27]. This mechanism can also occur in our case with the PFBT-P3HT diode. In fact, poor wetting of P3HT solutions on low-hydrophilicity surface results in the formation of edge-on oriented film [46]. This molecular organization is more suitable for the charge transport and the Π–Π orbital overlapping. The performance improvement of P3HT film crystallinity can also be in-

duced by sulfur-fluorine interactions between PFBT and P3HT, which leads to a denser molecular packing of P3HT, and a higher ordering of the organic semiconductor layer. These results have been investigated by Jurchescu and co-workers on fluorinated 5,11-bis(triethylsilylethynyl)anthradithiophene (diF-TESADT) films deposited on PFBT-Au electrodes [32,47]. Morphological effects such as roughness are also reported to affect the organic film growth and therefore electrical performances of the devices. In our configuration, the PFBT also leads to a decrease in the roughness of the surface. These multiple effects are proposed to be the origin of the performance improvement observed in the case of our PFBT-treated diodes.

### *3.2. Diode Rectifier on Flexible Substrate*

On another level and to demonstrate the possible flexibility of our devices, the Au-PFBT/P3HT/Al diode has been fabricated on flexible substrate, which is a cardboard paper provided by Centexbel (ref WO84). This paper has the advantage to possess a small roughness of about 1.4 nm (Figure 3a) due to a protective coating of silicone, and showed high stability to the solvent that are employed in the diode fabrication process. The paper was first placed in a primary vacuum oven at 100 °C for 1 h to degas the moisture present in the fibers. The diode was then fabricated on this substrate with the same process was detailed in the experimental part for silicon oxide substrate. In addition, this paper substrate is a release paper that can allow an easy transfer to all other flexible substrates such as textiles.

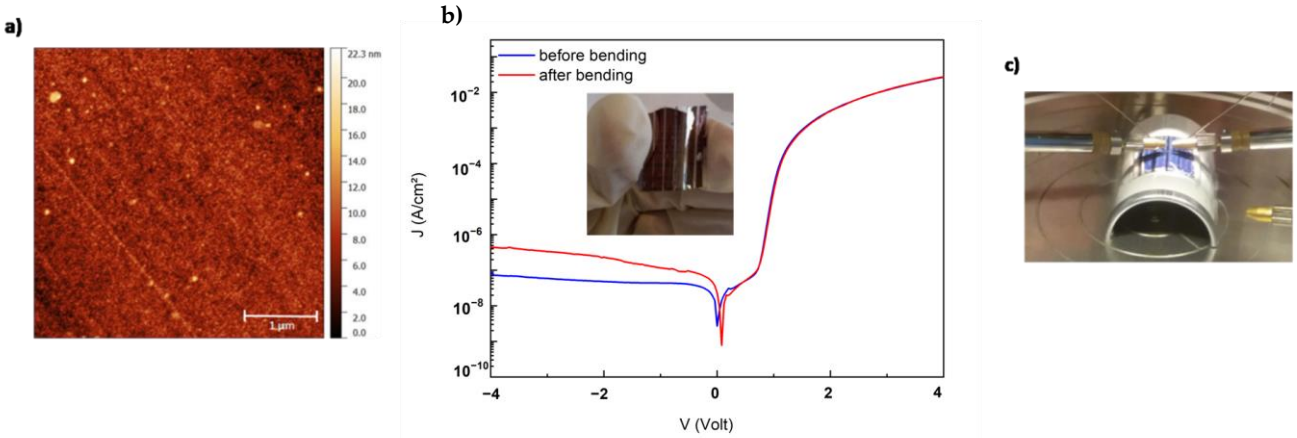


**Figure 3.** (**a**) AFM of the paper substrate, (**b**) J-V characteristic of the diode before and after bending, (**c**) photograph of measurement approach under bending (curvature radius 1.4 cm).

The electrical characteristic of the diode fabricated on the release paper is shown by Figure 3b. A density current of 0.026 A/cm$^2$ was obtained at 4 V and high rectification ratio r of 4 × 10$^5$ at ±4 V. The flexible diode rectifier is measured under bending tests (Figure 3c) with radius of 1.4 cm. The results show very good stability of the electrical characteristic except a little increase of the OFF current. This can be related to the direction of the bending that was made parallel to the aluminum electrode.

### *3.3. Frequency Response of the Rectifier Diode*

The frequency response of the diode rectifier was evaluated by LT-Spice simulation tools using the basic circuit rectifier shown in the inset of Figure 4. This circuit is composed of a function generator which provides the AC input signal for various frequencies, the diode rectifier, and the load capacitance. The load capacitance value needs to be higher than the capacitance of the diode to reduce the output voltage ripples [48], a value of 10 nF was chosen in our case. The parameters of the diode used in simulation are extracted experimentally by impedance spectroscopy measurements [43]. The obtained values for

the electrical equivalent circuit of the diode are $C_D$ = 174 pF (diode capacitance) and $R_D$ = 120 Ω (for the series resistance).

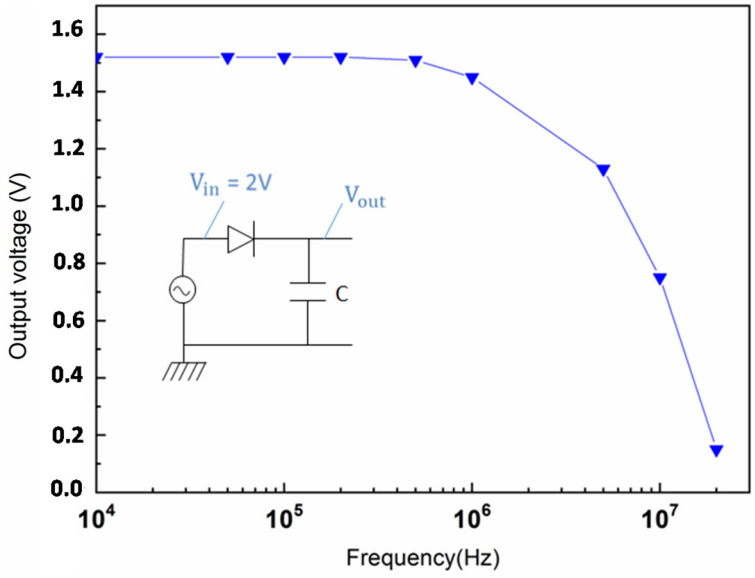


**Figure 4.** Frequency response of the P3HT diode rectifier.

The results of the simulation are shown in Figure 4. Under a 500 kHz, 2 V peak-to-peak oscillating input signal, an output DC voltage of 1.51 V was obtained, value that decreases to reach a DC output voltage of 0.15 when the input frequency increases to 20 MHz which is compatible with RFID applications (13.56 MHz). For energy harvesting, the frequency response of the diode can be improved by optimizing the device structure with reducing the capacitance of the diode and its resistance [43].

The Figure 5 represents the effects of the capacitance and the resistance of the diode on the frequency response. As it can be seen, minimizing the capacitance and series resistance is critical to achieving high frequency response up to Gigahertz, which corresponds to the theoretical equations [49] evaluating the frequency of the diode as proportional to these two parameters. The resistance of our P3HT diode rectifiers is in the order of 100 Ω and as can be seen by Figure 5b may lead to achieve FM, Wi-Fi band frequency. However, the capacitance of the diode needs to be further decreased to the range of pF value. Value that can be obtained with the design of diode rectifier with low area of active layer at the range of $5 \times 10^{-5}$ $cm^2$. In this case, a DC voltage of about 1 V is obtained at a frequency of 900 MHz. Even those values are small for energy harvesting systems, they can be increased by using other diode configurations, such as a voltage doubler or a Cockcroft multiplier [50,51].

As the rectenna is compatible with large surface configuration, one can imagine a system with an overlay of many rectenna devices to increase the power conversion efficiency.

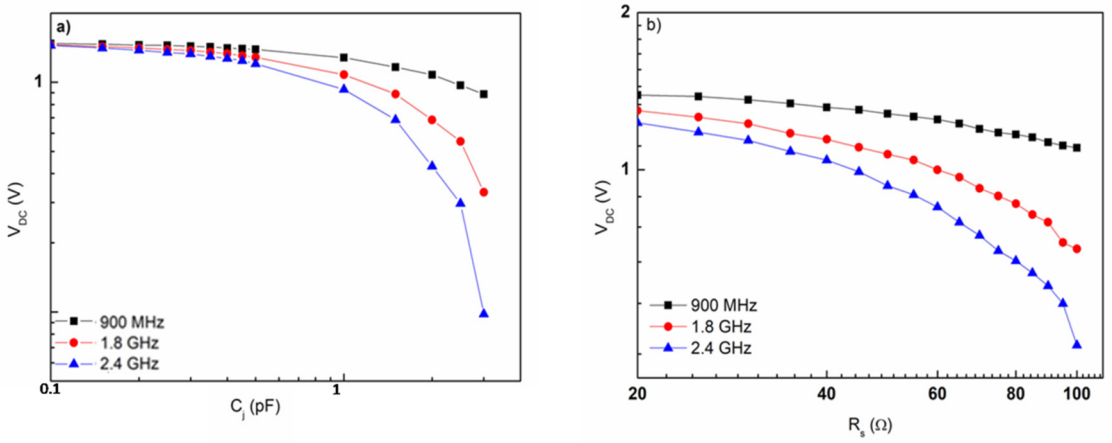


**Figure 5.** Influence of diode parameters on achieving high frequency response. (**a**) The effects of the capacitance, (**b**) the effects of the resistance.

## 4. Conclusions

In this study, high rectification ratio up to $10^6$ has been achieved for P3HT diode rectifier on silicon substrates and through the tuning of the work function of gold electrode anode by a self-assembled monolayer of PFBT. The P3HT rectifier diodes were also fabricated on flexible substrate (Centexbel release paper). They on paper demonstrated also a good rectification ratio and electrical stability under bending tests. Finally, to demonstrate the possibility of using our diodes in a rectenna circuits for the energy harvesting we study its frequency response. Operation frequency of 20 MHz can be achieved with the P3HT diode. This value can reach higher frequencies, in the GSM and Wi-Fi band by reducing the capacitance and series resistance of the diodes where continuous voltage of about 1 V can be recovered.

**Author Contributions:** Conceptualization, K.L., K.F.; methodology, K.L., K.F., D.G.; software, K.F.; validation, K.L., S.P. and R.B.; formal analysis, K.F., K.L., S.P.; investigation, K.F., S.P., D.G.; resources, K.L., K.F., S.P., D.G.; data curation, K.F.; writing—original draft preparation, K.F.; writing—review and editing, K.F., S.P. and K.L.; visualization, K.F., S.P. and K.L.; supervision, K.L., R.B.; project administration, K.L.; funding acquisition, K.L., R.B. All authors have read and agreed to the published version of the manuscript.

**Funding:** This work was financially supported by the European Project Interreg Luminoptex (grant number 1.1.45) and the French ANR Context project (grant number ANR-17-CE24-0013).

**Institutional Review Board Statement:** Not applicable.

**Informed Consent Statement:** Not applicable.

**Data Availability Statement:** The data presented in this study are available on request from the corresponding author.

**Acknowledgments:** This research work has been partially undertaken with the support of IEMN fabrication (CMNF) and characterization (PCMP) facilities. We thank the French National Nanofabrication Network RENATECH, and the IEMN cleanroom staff for their support. We also thank CENTEXBEL for the release paper supply.

**Conflicts of Interest:** The authors declare no conflict of interest. The funders had no role in the design of the study; in the collection, analyses, or interpretation of data; in the writing of the manuscript, or in the decision to publish the results.

## References


1. Semple, J.; Georgiadou, D.G.; Wyatt-Moon, G.; Gelinck, G.; Anthopoulos, T.D. Flexible diodes for radio frequency (RF) electronics: A materials perspective. *Semicond. Sci. Technol.* **2017**, *32*, 123002. [CrossRef]
2. Sani, N.; Robertsson, M.; Cooper, P.; Wang, X.; Svensson, M.; Ersman, P.A.; Norberg, P.; Nilsson, M.; Nilsson, D.; Liu, X.; et al. All-printed diode operating at 1.6 GHz. *Proc. Natl. Acad. Sci. USA* **2014**, *111*, 11943–11948. [CrossRef] [PubMed]
3. Facchetti, A. Printed diodes operating at mobile phone frequencies. *Proc. Natl. Acad. Sci. USA* **2014**, *111*, 11917–11918. [CrossRef] [PubMed]
4. Wang, H.; Ji, Z.; Shang, L.; Chen, Y.; Lu, C.; Li, D.; Peng, Y.; Liu, M. Low-cost 13.56MHz Rectifier Based on Organic Diode, MRS Online Proceedings Library Archive. *MRS Proc.* **2012**, *1402*, 13–18. [CrossRef]
5. Smith, J.; Hamilton, R.; Heeney, M.; De Leeuw, D.M.; Cantatore, E.E.; Anthony, J.; McCulloch, I.; Bradley, D.; Anthopoulos, T. High-performance organic integrated circuits based on solution processable polymer-small molecule blends. *Appl. Phys. Lett.* **2008**, *93*, 253301. [CrossRef]
6. Holliday, S.; Ashraf, R.S.; Wadsworth, A.; Baran, D.; Yousaf, S.A.; Nielsen, C.B.; Tan, C.-H.; Dimitrov, S.; Shang, Z.; Gasparini, N.; et al. High-efficiency and air-stable P3HT-based polymer solar cells with a new non-fullerene acceptor. *Nat. Commun.* **2016**, *7*, 11585. [CrossRef] [PubMed]
7. Chandrasekaran, N.; Liu, A.; Kumar, A.; McNeill, C.R.; Kabra, D. Effect of regioregularity on recombination dynamics in inverted bulk heterojunction organic solar cells. *J. Phys. D Appl. Phys.* **2017**, *51*, 015501. [CrossRef]
8. Seon, H.; Kim, B.; Kang, J. Characteristic of an Organic Photodetector fabricated with P3HT: ICBA blending materials for Indirect X-ray Detection. *IEEE Trans. Nucl. Sci.* **2016**, *64*, 1739–1743. [CrossRef]
9. Jeong, J.W.; Park, Y.W.; Park, T.H.; Choi, J.H.; Choi, H.J.; Song, E.H.; Lee, J.I.; Chu, H.Y.; Ju, B.K. The emission properties of integrated organic light emitting diodes with organic photo sensor for emotional lighting applications. *IEEE Electron Device Lett.* **2011**, *32*, 348–350. [CrossRef]
10. Chun, J.-Y.; Han, J.-W.; Kim, T.-W.; Seo, D.-S. Enhancement of organic light-emitting diodes efficiency using carbon nanotube doped hole-injection layer on the Al-doped ZnO anode. *ECS Solid State Lett.* **2012**, *1*, R13–R15. [CrossRef]
11. Yasin, M.; Tauqeer, T.; Karimov, K.S.; San, S.E.; Kösemen, A.; Yerli, Y.; Tunc, A.V. P3HT:PCBM blend based photo organic field effect transistor. *Microelectron. Eng.* **2014**, *130*, 13–17. [CrossRef]
12. Han, S.; Zhuang, X.; Shi, W.; Yang, X.; Li, L.; Yu, J. Poly(3-hexylthiophene)/polystyrene (P3HT/PS) blends based organic field-effect transistor ammonia gas sensor. *Sens. Actuators B Chem.* **2015**, *225*, 10–15. [CrossRef]
13. Hong, C.T.; Kang, Y.H.; Ryu, J.; Cho, S.Y.; Jang, K.-S. Spray-printed CNT/P3HT organic thermoelectric films and power generators. *J. Mater. Chem. A* **2015**, *3*, 21428–21433. [CrossRef]
14. Jang, E.; Poosapati, A.; Madan, D. Enhanced thermoelectric properties of F4TCNQ doped P3HT and its use as a binder for Sb2Te3 based printed thermoelectric films. *ACS Appl. Energy Mater.* **2018**, *1*, 1455–1462. [CrossRef]
15. Qian, C.; Sun, J.; Kong, L.-A.; Gou, G.; Yang, J.; He, J.; Gao, Y.; Wan, Q. Artificial synapses based on in-plane gate organic electrochemical transistors. *ACS Appl. Mater. Interfaces* **2016**, *8*, 26169–26175. [CrossRef] [PubMed]
16. Qian, C.; Kong, L.-A.; Yang, J.; Gao, Y.; Sun, J. Multi-gate organic neuron transistors for spatiotemporal information processing. *Appl. Phys. Lett.* **2017**, *110*, 083302. [CrossRef]
17. Lin, C.-Y.; Tsai, C.-H.; Lin, H.-T.; Chang, L.-C.; Yeh, Y.-H.; Pei, Z.; Peng, Y.-R.; Wu, C.-C. High-frequency polymer diode rectifiers for flexible wireless power-transmission sheets. *Org. Electron.* **2011**, *12*, 1777–1782. [CrossRef]
18. Kang, C.-M.; Kim, S.; Hong, Y.; Lee, C. Frequency analysis on poly(3-hexylthiopene) rectifier using impedance spectroscopy. *Thin Solid Films* **2009**, *518*, 889–892. [CrossRef]
19. Kim, K.; Koo, J.; Lee, J.; Yang, Y.S.; You, I.K.; Noh, Y.Y. Variations in the electric characteristics of an organic schottky diode with the P3HT thickness. *J. Korean Phys. Soc.* **2010**, *57*, 124–127. [CrossRef]
20. Kim, S.; Cho, H.; Hong, Y.; Lee, C. Effect of electrode area on high speed characteristics over 1 MHz of poly (3-hexylthiophene-2, 5-diyl) diode with Inkjet-printed Ag electrode. *Mol. Cryst. Liq. Cryst.* **2009**, *513*, 256–261. [CrossRef]
21. Cao, M.; Hyun, W.J.; Francis, L.F.; Frisbie, C.D. Inkjet-printed, self-aligned organic Schottky diodes on imprinted plastic substrates. *Flex. Print. Electron.* **2020**, *5*, 015006. [CrossRef]
22. Koch, N.; Kahn, A.; Ghijsen, J.; Pireaux, J.-J.; Schwartz, J.; Johnson, R.L.; Elschner, A. Conjugated organic molecules on metal versus polymer electrodes: Demonstration of a key energy level alignment mechanism. *Appl. Phys. Lett.* **2003**, *82*, 70–72. [CrossRef]
23. Diao, L.; Frisbie, C.D.; Schroepfer, D.D.; Ruden, P.P. Electrical characterization of metal/pentacene contacts. *J. Appl. Phys.* **2007**, *101*, 014510. [CrossRef]
24. Song, D.-S.; Roh, J.; Lee, C.; Shin, D.Y.; Bae, J.-H.; Kim, H. Hole injection in N-type organic semiconductors by tuning metal work function with functional self-assembled monolayers. *J. Nanosci. Nanotechnol.* **2017**, *17*, 3378–3381. [CrossRef]
25. Kang, C.M.; Hong, Y.; Lee, C. Frequency performance optimization of flexible pentacene rectifier by varying the thickness of active layer. *Jpn. J. Appl. Phys.* **2010**, *49*, 05EB07. [CrossRef]
26. Hong, J.-P.; Park, A.-Y.; Lee, S.; Kang, J.; Shin, N.; Yoon, D.Y. Tuning of Ag work functions by self-assembled monolayers of aromatic thiols for an efficient hole injection for solution processed triisopropylsilylethynyl pentacene organic thin film transistors. *Appl. Phys. Lett.* **2008**, *92*, 143311. [CrossRef]

27. Fenwick, O.; Van Dyck, C.; Murugavel, K.; Cornil, D.; Reinders, F.; Haar, S.; Mayor, M.; Cornil, J.; Samorì, P. Modulating the charge injection in organic field-effect transistors: Fluorinated oligophenyl self-assembled monolayers for high work function electrodes. *J. Mater. Chem. C* **2015**, *3*, 3007–3015. [CrossRef]
28. Kang, C.-M.; Wade, J.; Yun, S.; Lim, J.; Cho, H.; Roh, J.; Lee, H.; Nam, S.; Bradley, D.D.C.; Kim, J.-S. 1 GHz pentacene diode rectifiers enabled by controlled film deposition on SAM-treated Au anodes. *Adv. Electron. Mater.* **2015**, *2*, 1500282. [CrossRef]
29. Kim, J.; Rim, Y.S.; Liu, Y.; Serino, A.C.; Thomas, J.C.; Chen, H.; Yang, Y.; Weiss, P.S. Interface control in organic electronics using mixed monolayers of carboranethiol isomers. *Nano Lett.* **2014**, *14*, 2946–2951. [CrossRef]
30. Chen, J.; Gathiaka, S.; Wang, Z.; Thuo, M.M. Role of molecular dipoles in charge transport across large area molecular junctions delineated using isomorphic self-assembled monolayers. *J. Phys. Chem. C* **2017**, *121*, 23931–23938. [CrossRef]
31. Cao, J.; Yin, J.; Yuan, S.; Zhao, Y.; Li, J.; Zheng, N. Thiols as interfacial modifiers to enhance the performance and stability of perovskite solar cells. *Nanoscale* **2015**, *7*, 9443–9447. [CrossRef] [PubMed]
32. Li, S.; Guerin, D.; Lenfant, S.; Lmimouni, K. Optimization of pentacene double floating gate memories based on charge injection regulated by SAM functionalization. *AIP Adv.* **2018**, *8*, 25110. [CrossRef]
33. Asadi, K.; Wu, Y.; Gholamrezaie, F.; Rudolf, P.; Blom, P.W.M. Single-layer pentacene field-effect transistors using electrodes modified with self-assembled monolayers. *Adv. Mater.* **2009**, *21*, 4109–4114. [CrossRef]
34. Gundlach, D.J.; Royer, J.E.; Park, S.K.; Subramanian, S.; Jurchescu, O.D.; Hamadani, B.H.; Moad, A.J.; Kline, R.; Teague, L.C.; Kirillov, O.; et al. Contact-induced crystallinity for high-performance soluble acene-based transistors and circuits. *Nat. Mater.* **2008**, *7*, 216–221. [CrossRef] [PubMed]
35. Choi, S.; Larrain, F.A.; Chou, W.-F.; Wang, C.-Y.; Fuentes-Hernandez, C.; Kippelen, B. Self-forming electrode modification in organic field-effect transistors. *J. Mater. Chem. C* **2016**, *4*, 8297–8303. [CrossRef]
36. Devynck, M.; Tardy, P.; Wantz, G.; Nicolas, Y.; Vellutini, L.; Labrugère, C.; Hirsch, L. Cumulative effects of electrode and dielectric surface modifications on pentacene-based transistors. *Appl. Phys. Lett.* **2012**, *100*, 053308. [CrossRef]
37. Kim, C.H.; Hlaing, H.; Carta, F.; Bonnassieux, Y.; Horowitz, G.; Kymissis, I. Templating and charge injection from copper electrodes into solution-processed organic field-effect transistors. *ACS Appl. Mater. Interfaces* **2013**, *5*, 3716–3721. [CrossRef]
38. Nagase, T.; Abe, S.; Kobayashi, T.; Kimura, Y.; Hamaguchi, A.; Ikeda, Y.; Naito, H. Solution-processed organic field-effect transistors based on dinaphthothienothiophene precursor with chemically modified electrodes. *J. Phys. Conf. Ser.* **2017**, *924*, 12008. [CrossRef]
39. Li, S.; Guerin, D.; Lmimouni, K. Improving performance of OFET by tuning occurrence of charge transport based on pentacene interaction with SAM functionalized contacts. *Microelectron. Eng.* **2018**, *195*, 62–67. [CrossRef]
40. Shih, C.-C.; Chiu, Y.-C.; Lee, W.-Y.; Chen, J.-Y.; Chen, W.-C. Conjugated polymer nanoparticles as nano floating gate electrets for high performance nonvolatile organic transistor memory devices. *Adv. Funct. Mater.* **2015**, *25*, 1511–1519. [CrossRef]
41. Nijhuis, C.A.; Reus, W.F.; Whitesides, G.M. Mechanism of rectification in tunneling junctions based on molecules with asymmetric potential drops. *J. Am. Chem. Soc.* **2010**, *132*, 18386–18401. [CrossRef]
42. Thuo, M.M.; Reus, W.F.; Nijhuis, C.A.; Barber, J.R.; Kim, C.; Schulz, M.D.; Whitesides, G.M. Odd-even effects in charge transport across self-assembled monolayers. *J. Am. Chem. Soc.* **2011**, *9*, 2962–2975. [CrossRef]
43. Ferchichi, K.; Pecqueur, S.; Guerin, D.; Bourguiga, R.; Lmimouni, K. Organic doped diode rectifier based on parylene-electronic beam lithogrpahy process for radio frequency applications. *Org. Electron.* **2021**, *97*, 106266. [CrossRef]
44. Kuzumoto, Y.; Kitamura, M. Work function of gold surfaces modified using substituted benzenethiols: Reaction time dependence and thermal stability. *Appl. Phys. Express* **2014**, *7*, 035701. [CrossRef]
45. Tatara, S.; Kuzumoto, Y.; Kitamura, M. Surface properties of substituted-benzenethiol monolayers on gold and silver: Work function, wettability, and surface tension. *Jpn. J. Appl. Phys.* **2016**, *55*, 03DD02. [CrossRef]
46. Pandey, R.K.; Mishra, R.; Tiwari, P.; Prakash, R. Interface engineering for enhancement in performance of organic/inorganic hybrid heterojunction diode. *Org. Electron.* **2017**, *45*, 26–32. [CrossRef]
47. Jurchescu, O.D.; Hamadani, B.H.; Xiong, H.D.; Park, S.K.; Subramanian, S.; Zimmerman, N.M.; Anthony, J.E.; Jackson, T.N.; Gundlach, D.J. Correlation between microstructure, electronic properties and flicker noise in organic thin film transistors. *Appl. Phys. Lett.* **2008**, *92*, 132103. [CrossRef]
48. Steudel, S.; De Vusser, S.; Myny, K.; Lenes, M.; Genoe, J.; Heremans, P. Comparison of organic diode structures regarding high-frequency rectification behavior in radio-frequency identification tags. *J. Appl. Phys.* **2006**, *99*, 114519. [CrossRef]
49. Chasin, A.; Volskiy, V.; Libois, M.; Ameys, M.; Nag, M.; Rockele, M.; Myny, K.; Steudel, S.; Schols, S.; Vandenbosch, G.A.E.; et al. An integrated a-IGZO UHF energy harvester for passive RFID tags. *IEEE Trans. Electron Devices* **2014**, *61*, 3289–3295. [CrossRef]
50. Kim, S.; Cho, J.-H.; Hong, S.-K. A full wave voltage multiplier for RFID transponders. *IEICE Trans. Commun.* **2008**, *91*, 388–391. [CrossRef]
51. Jaiwanglok, A.; Eguchi, K.; Julsereewong, A.; Pannil, P. Alternative of high voltage multipliers utilizing Cockcroft–Walton multiplier blocks for 220 V and 50 Hz input. *Energy Rep.* **2020**, *6*, 909–913. [CrossRef]